Research Square

Preprints are preliminary reports that have not undergone peer review.
They should not be considered conclusive, used to inform clinical practice,
or referenced by the media as validated information.

Bio-Stabilized Copper Nanoclusters Enable Highly Selective Aerobic Alcohol Oxidation in Water

Vahideh Sarvari
University of Birjand
Reihaneh Malakooti
rmalakooti@birjand.ac.ir
University of Birjand
Davoud Mousavi
University of Birjand

Article

Keywords: BSA–Cu nanoclusters, Aerobic oxidation, Benzyl alcohol, Copper nanocatalyst, Isobutyraldehyde cocatalyst

Posted Date: November 5th, 2026

DOI: https://doi.org/10.21203/rs.3.rs-11418858/v1

License: This work is licensed under a Creative Commons Attribution 4.0 International License.
Read Full License

Additional Declarations: No competing interests reported.

Bio-Stabilized Copper Nanoclusters Enable Highly Selective Aerobic Alcohol Oxidation in Water

Vahideh Sarvari[a], Reihaneh Malakooti[a*], Davoud Mousavi[a]
[a] Department of Chemistry, Faculty of Science, University of Birjand, Birjand, Iran.
Corresponding author: Reihaneh Malakooti, rmalakooti@birjand.ac.ir.

Abstract

Water-soluble bovine serum albumin-stabilized copper nanoclusters (BSA–Cu NCs) were synthesized and fully characterized by FT-IR, UV–Vis, TEM, XPS, photoluminescence spectroscopy, ICP, and TGA. The ultrasmall nanoclusters (1.7 ± 0.5 nm), predominantly containing Cu^0 species, exhibited high structural stability and strong ligand-to-metal charge transfer features. The BSA–Cu NCs demonstrated excellent catalytic performance in the aerobic oxidation of a wide range of primary and secondary alcohols under mild conditions (25 °C, water, air or O_2), affording the corresponding carbonyl compounds with >99 % selectivity. Studies on optimization showed that catalyst loading, oxygen flow rate, and isobutyraldehyde as a cocatalyst are all important for getting quantitative conversions in a short amount of time. Spectroscopic analyses and radical-trapping experiments substantiate a Cu(II)/Cu(I) redox-mediated radical pathway, while dismissing the generation of peroxo or superoxo copper species. The catalyst kept working over many cycles with very little damage to its structure. Compared with previously reported copper-based systems, the BSA–Cu NCs offer a sustainable, efficient, and environmentally benign platform for aerobic alcohol oxidation in aqueous media.

Keywords: BSA–Cu nanoclusters, Aerobic oxidation, Benzyl alcohol, Copper nanocatalyst, Isobutyraldehyde cocatalyst

Introduction

In the homogeneous nanocatalyst approach, nanoparticles derived from transition metals are dispersed in the reaction medium in the form of colloids (suspended particles). An organic solvent, and/or aqueous solvent, is usually used in this kind of catalytic system. A stabilizing agent is often added to retain nanoparticles separately. A good stabilizer keeps the nanocatalyst stable during the catalytic process and prevents it from self-aggregating without lowering its catalytic activity. Moreover, the nanoparticles can be separated from the final reaction products after completion of the reaction[1].

Enzymes are biological catalysts that accelerate the rates of biochemical reactions in living cells and are therefore referred to as vital catalysts. In recent years, enzymes have gained significant importance in chemistry as green catalysts. Compared with conventional chemical catalysts, enzymes offer several advantages, including high selectivity in complex reaction mixtures, high product purity with minimal or no by-product formation, mild reaction conditions, low production costs, and exceptional chemo-, regio-, and stereoselectivity. The catalytic properties of enzymes attracted attention even before their molecular structures were fully elucidated. Enzymes operate according to the same fundamental principles as other catalysts in chemistry; they do not alter the Gibbs free energy of a reaction. Rather, similar to chemical catalysts, they either modify the reaction mechanism or increase the effective concentration of the substrate through pre-concentration at their active sites, thereby reducing the overall activation energy of the reaction. The catalytic activity of enzymes is

influenced by several factors, among which pH, substrate concentration, and temperature are the most critical[2], [3].

Bovine serum albumin (BSA), also known as Fraction V, is a 66,463 Da protein widely used as an inexpensive and commercially available stabilizing agent for nanocluster synthesis. Possessing seventeen disulfide bonds and one free cysteine residue, BSA provides a strong stabilizing framework for nanocluster formation [4]. Moreover, the presence of diverse functional groups (–NH, –SH, –OH, –COOH) enables effective interaction with metal ions, facilitating both nucleation and stabilization processes. However, the efficacy of BSA as a synthetic template is intrinsically linked to its pH-responsive conformational dynamics. Recent evidence indicates that pH-induced shifts trigger a transition from native α-helices to β-sheet-rich structures, accompanied by a significant expansion of the tertiary architecture—as reflected in increased ANS-binding accessibility and structural disorder within the F and B domains. These findings, which necessitate an expansion of the classical Foster model[5], are critical for modulating the nucleation and stabilization of nanoclusters through the precise tuning of protein-metal interactions.

Over recent decades, the synthesis of heavy-metal nanoclusters has undergone substantial development. These clusters, with sizes below 2 nm and consisting of several to hundreds of atoms, act as a bridge between traditional organometallic compounds and crystalline metal nanoparticles. Their unique physicochemical properties clearly distinguish them from isolated atoms as well as bulk materials [5]. Owing to their ultrasmall size, favorable biocompatibility, high stability, and luminescent properties, these nanoclusters have attracted considerable interest for applications in catalysis and biomedicine [4]. Because of their distinct energy levels, metal nanoclusters show electronic transitions in the conduction band that are very similar to those found in molecular systems. Their unique physicochemical characteristics, such as their use in the synthesis of labeled cells and catalytic activities, are supported by this molecule-like electronic structure [6]. Metal nanoclusters are very appealing for catalytic and biomedical applications because of their favorable characteristics over quantum dots, including reduced toxicity and chemically accessible surfaces that are rich in functional groups[7]. Their catalytic performance in particular is directly attributed to their extremely small dimensions and the resulting electronic and surface effects [8], Some studies have highlighted their unique potential as environmentally benign catalysts in a variety of important chemical transformations. Notable examples include the synthesis of methanol from syngas, hydrogen production from methanol gas[9]. methanol oxidation reactions[10], and the selective hydrogenation of aldehydes and ketones[11]. Some reports have demonstrated the exceptionally high catalytic activity of gold nanoclusters, such as Au25, Au38, Au55, and Au144 [8], In addition to cluster size, several other parameters—including coordination number, charge state, metal–support interactions, and bond length—play crucial roles in determining the efficiency and selectivity of these catalytic reactions[12]. However, owing to the high cost of ultrasmall gold nanoclusters, copper nanoclusters have emerged as attractive alternative catalysts and have therefore received increasing attention [13].

Copper, owing to its lower cost and greater natural abundance compared to gold, represents a highly attractive alternative catalyst[14], [15]. Indeed, the use of larger-sized copper nanoparticles has been reported in a variety of catalytic reactions, including methanol synthesis and oxidation, acetylene hydrogenation[9], and the hydroxylation of phenol using hydrogen peroxide[16]. Copper in the form of coordination complexes is of considerable importance as a catalyst in chemical research. Depending on the system, these copper-based catalysts can operate under either homogeneous or heterogeneous conditions and are capable of oxidizing a wide range of organic

substrates. In 2013, water-soluble, fluorescent copper nanoclusters were synthesized by the group of Wang Chan and co-workers for catalytic applications as well as biomedical purposes [4].

Copper has a high catalytic activity that is similar to that of noble metals like Ru, Au, and Pd [17]. It can also prevent become inactive the catalysts by forming stabilizing interactions between the metal center and heteroatoms [18]. On the other hand, owing to its lower oxidation potential (Cu^{2+}/Cu E_{red}= +0.34 V) compared to noble metals, copper generally requires suitable ligands to facilitate efficient electron transfer and thereby enhance the oxidation of alcohols. Ligands that are traditionally employed for this purpose include 2,2′-bipyridine (bpy), 1,10-phenanthroline (phen), and their derivatives[19]. For example, Marko and co-workers[20] employed phenanthroline as a ligand in CuCl-based catalytic systems in toluene for the oxidation of alcohols. Subsequently, Sheldon and co-workers[21] developed a ternary CuBr/TEMPO/O_2 catalytic system, incorporating bipyridine as the ligand in a CH_3CN/H_2O solvent mixture, for the selective oxidation of primary benzylic alcohols to the corresponding aldehydes. Subsequently, the Cu/ligand/TEMPO catalytic system was modified by Knochel and co-workers[22]. In the redesigned system, $CuBr{\cdot}Me_2S$ served as the catalyst, while replacement of bipyridine with a fluoroalkyl ligand created a fluorinated biphasic medium ($C_8F_{17}Br$/PhCl) exhibiting remarkably enhanced catalytic activity. However, due to the hydrophobic nature of these ligands, oxidation reactions generally require organic solvents or mixed solvent systems. Water, being abundant, non-toxic, and capable of enhancing both selectivity and catalytic activity in oxidation reactions, has attracted growing attention as a green solvent[11]. Consequently, there is an increasing trend toward the development and use of water-soluble ligands in copper-catalyzed oxidation systems [22].

Copper-based systems have emerged as effective catalysts for aerobic alcohol oxidation, particularly when combined with TEMPO and appropriate ligands. Semmelhack and co-workers first demonstrated practical copper/TEMPO-mediated aerobic alcohol oxidation in 1984, although the system was largely restricted to primary alcohols[23]. Subsequent ligand-assisted Cu/TEMPO systems, including $CuBr_2$/2,2′-bipyridine, enabled highly selective oxidation of primary alcohols while suppressing overoxidation to carboxylic acids[24]. Subsequent systematic optimization of copper catalysts, ligands, bases, and solvents led to the development of the (bpy)CuI/TEMPO system, which showed broad functional-group tolerance and high selectivity toward both primary and secondary alcohols, including unprotected diols[25]. Despite these advances, molecular copper catalysts typically require carefully engineered ligand environments and organic reaction media, motivating the development of more robust copper-based platforms for selective aerobic oxidation under aqueous conditions.

Herein, we develop water-soluble bovine serum albumin-stabilized copper nanoclusters (BSA–Cu NCs) as a heterogeneous catalyst for highly selective aerobic alcohol oxidation in water. The bio-stabilized Cu nanoclusters enable efficient oxidation of primary and secondary alcohols under mild conditions using air or O_2, while maintaining high selectivity toward carbonyl products and excellent recyclability. Mechanistic studies reveal a Cu(I)/Cu(II)-mediated radical pathway, highlighting BSA–Cu NCs as a sustainable platform for selective aerobic oxidation in aqueous media.

Materials and Methods

Bovine serum albumin (BSA, Fraction V, molecular weight 66.5 kg mol^{-1}), hydrazine hydrate (100%), copper(II) sulfate pentahydrate ($CuSO_4{\cdot}5H_2O$), isobutyraldehyde, benzyl alcohol, sodium hydroxide, ethyl acetate, and diethyl ether were purchased from Merck. All chemicals were used as received without further purification. Deionized water was used in all experiments where required.

Instrumentation

X-ray photoelectron spectroscopy (XPS) measurements were performed using a Specs EA10 Plus spectrometer. Inductively coupled plasma (ICP) analysis was conducted on a Perkin Elmer OPTIMA 7300 DV instrument. Transmission electron microscopy (TEM) images were obtained with a Philips CM30 microscope operated at an acceleration voltage of 100 kV. UV–visible absorption spectra were recorded on a Shimadzu UV-Vis 2510 PC spectrophotometer. Thermogravimetric analysis (TGA) was carried out using a Shimadzu TGA-50 instrument with a heating rate of 5 °C min^{-1} over the temperature range 25–400 °C. Photoluminescence (PL) measurements were performed using a Shimadzu RF-530 fluorescence spectrometer at room temperature (≈ 300 K). Fourier-transform infrared (FT-IR) spectra were recorded on a Bruker VERTEX 70 spectrometer (Germany).

Synthesis of Copper Nanoclusters

In a standard synthesis, 100 mg of bovine serum albumin (BSA) was incorporated into 5 mL of a 5 mM copper sulfate aqueous solution while being stirred continuously at room temperature. After mixing for 10 minutes, a blue gel formed. This shows that copper ions are coordinating with the functional groups of BSA, such as hydroxyl, amino, and sulfur-containing groups. After that, 1 M sodium hydroxide solution was added drop by drop to the solution to bring the pH up to 12. As a reducing agent, 1 mL of hydrazine hydrate (100%) was added to the reaction mixture after the pH was changed. The reaction was then allowed to proceed under continuous stirring at room temperature for 4 h, during which the solution gradually transformed into a light yellow colloidal dispersion, indicating the successful formation of copper nanoclusters (CuNCs). The synthesized Cu nanocluster catalyst was stored in a refrigerator for further use (Figure 1) [4].

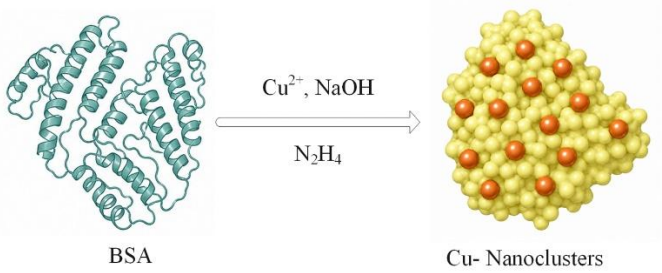


Figure 1. General Procedure for the Aerobic Oxidation of Alcohols Using Water-Soluble Copper Nanoclusters [4].

The aerobic oxidation of alcohols was carried out using either air or molecular oxygen as the oxidant at a constant flow rate of 5 mL min^{-1}. All reactions were performed at room temperature in a 5 mL two-neck round-bottom flask. In a typical experiment, the reaction mixture consisted of 1.38 mol% of the copper nanocluster catalyst, 0.05 mL (0.5 mmol) of the alcohol substrate, 3 mL of deionized water, and 0.8 mL (8 mmol) of isobutyraldehyde as the sacrificial co-reductant. The reaction was stirred continuously under an air or oxygen atmosphere and was typically completed within 1.5 h. Upon completion, the reaction mixture was extracted with ethyl acetate , and the organic phase was collected for further analysis. For certain alcohol substrates, depending on their intrinsic reactivity toward the copper nanocluster catalyst, the reaction time was adjusted accordingly and could be either shortened or prolonged.

Discussion and Conclusion

Bovine serum albumin-stabilized copper nanoclusters (BSA–Cu NCs) were successfully produced. The structure and morphology of as-synthesized materials were well characterized. The FT-IR spectrum provides clear evidence for the successful formation of water-soluble copper nanoclusters (CuNCs) stabilized by BSA (Figure 2). In the spectrum of pure BSA used as the ligand (Fig. 2a), the characteristic absorption band at 3439 cm^{-1} is attributed to the stretching vibrations of –OH and N–H groups, corresponding to the amide A region. The absorption band observed at 1649 cm^{-1}, located in the amide I region, is assigned to the C=O stretching vibration of the peptide backbone. In addition, the band appearing at 1544 cm^{-1} in the amide II region is associated with the N–H bending vibration. A comparison between the FT-IR spectrum of BSA-stabilized copper nanoclusters (Fig. 2b) and that of pristine BSA reveals the appearance of new absorption bands at 1096, 955, and 914 cm^{-1}, which can be attributed to the interaction between BSA functional groups and Cu(0) species. Furthermore, the characteristic absorption bands corresponding to –OH, C=O, and N–H groups in the CuNCs spectrum exhibit noticeable shifts toward lower wavenumbers, indicating the formation of coordination bonds between copper atoms and BSA as the stabilizing ligand. Moreover, the –NH stretching vibration appears as a broadened band, which is likely due to its overlap and interaction with the –OH stretching mode. This observation is in good agreement with previously reported reference spectra and further supports the successful coordination of copper nanoclusters with BSA [26].

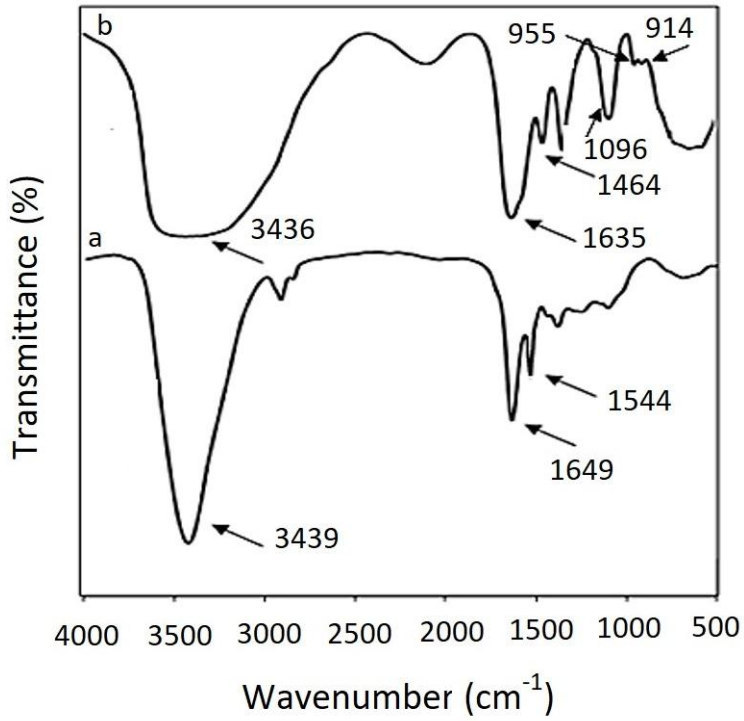


Figure 2. FT-IR spectra of (a) pristine bovine serum albumin (BSA) and (b) BSA-stabilized copper nanoclusters (BSA–Cu NCs) in the solution state.

Ultraviolet–visible (UV–Vis) spectroscopy, also referred to as absorption spectroscopy in the ultraviolet–visible region, was employed to investigate the electronic features of the synthesized copper nanoclusters. As shown in Figure 3, the UV–Vis spectra were recorded in the wavelength range of 220–450 nm, where Fig. 3a corresponds to the absorption spectrum of copper sulfate salt ($CuSO_4 \cdot 5H_2O$), (Fig. 3b) represents the spectrum of the copper nanoclusters (CuNCs), and curve Fig. 3c corresponds to the BSA ligand. The characteristic absorption band observed at approximately 230 nm in Fig. 3a is attributed to the $CuSO_4 \cdot 5H_2O$ precursor and is in good agreement with previously

reported reference spectra[27]. The UV-Vis spectrum of pure BSA Fig. 3c exhibits a distinct absorption peak at 280 nm, which arises from the presence of aromatic amino acids—namely tryptophan, tyrosine, and phenylalanine—within the protein structure. This absorption is associated with $\pi \rightarrow \pi^*$ electronic transitions of the aromatic rings and is consistent with reported UV–Vis data for BSA[28]. Notably, the spectrum of the BSA-stabilized copper nanoclusters Fig. 3b displays two absorption bands centered at approximately 280 nm and 230 nm. The absorption at 280 nm, which appears with reduced intensity compared to that of pristine BSA, confirms the presence of BSA on the surface of the copper nanoclusters and indicates strong interactions between the protein functional groups (such as –NH, –SH, and –COOH) and the metallic nanocluster core[29]. Furthermore, the emergence of an absorption band at lower wavelengths, around 230 nm, can be attributed to ligand-to-metal charge transfer (LMCT) transitions, providing additional evidence for the successful coordination between BSA and the copper nanoclusters.

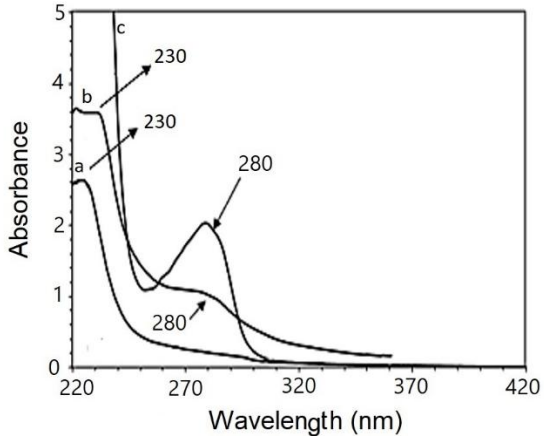


Figure 3. UV–Vis absorption spectra of (a) $CuSO_4 \cdot 5H_2O$, (b) BSA-stabilized copper nanoclusters (BSA–Cu NCs), and (c) pristine bovine serum albumin (BSA), recorded in the wavelength range of 220–450 nm.

Transmission electron microscopy (TEM) was employed to investigate the morphology and size distribution of the synthesized copper nanoclusters (Figure 4). The TEM image shown in Fig. 4a corresponds to water-soluble copper nanoclusters (Cu NCs). To obtain reliable particle size statistics, 100 nanoclusters were randomly selected from the TEM micrographs and analyzed. As clearly observed, the Cu nanoclusters exhibit a narrow size distribution with an average particle diameter of 1.7 ± 0.5 nm, confirming the formation of ultrasmall nanoclusters rather than larger copper nanoparticles. Also, the histogram of the particle size distribution shown in Fig. 4b follows a normal (Gaussian) distribution. This means that the nanoclusters were formed evenly and stayed stable during synthesis[30], [31].

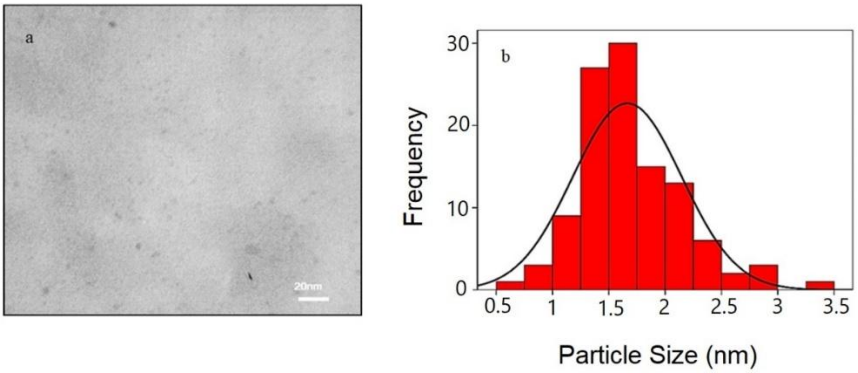


Figure 4. (a) Transmission electron microscopy (TEM) image, and (b) Particle size distribution histogram of BSA-stabilized copper nanoclusters (BSA–Cu NCs).

In the present study, XPS was employed to determine the oxidation state of copper in the water-soluble copper nanoclusters (Figure 5). The high-resolution Cu 2p XPS spectrum (Fig. 5) exhibits two characteristic peaks. The dominant peak located at a binding energy of 932.3 eV, assigned to the Cu $^2P_{3/2}$ orbital, is characteristic of metallic copper (Cu^0) [32]. A weaker peak observed at 953 eV, suggests the presence of a minor fraction of Cu^{2+} species in the nanocluster composition[33]. The coexistence of Cu^0 and trace Cu^{2+} can be attributed to partial surface oxidation or coordination interactions with the BSA ligand. Overall, the XPS results provide compelling evidence for the successful formation of BSA-stabilized copper nanoclusters, predominantly containing Cu^0 species, with surface-coordinated organic ligands that contribute to the stability and water solubility of the nanoclusters.

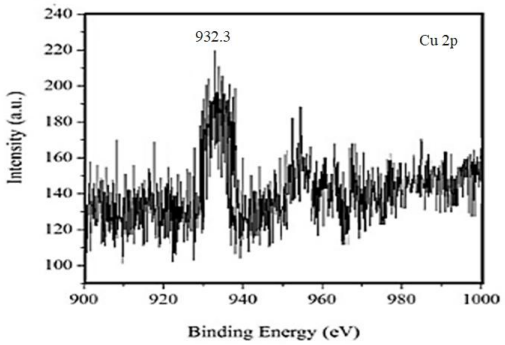


Figure 5. X-ray photoelectron spectroscopy (XPS) spectrum of BSA-stabilized copper nanoclusters (BSA–Cu NCs): High-resolution Cu 2p spectrum.

The water-soluble copper nanoclusters exhibited pronounced photoluminescence characteristics, with distinct excitation (Ex) and emission (Em) maxima at 534 nm and 632 nm, respectively (Figure 6), aligning well with previously documented literature values [4]. The presence of the characteristic emission peak further substantiates the successful synthesis of BSA-stabilized copper nanoclusters (BSA–Cu NCs). Additionally, due to the protein shell, the BSA-coated copper nanoclusters exhibit exceptional biocompatibility and minimal cytotoxicity. Consequently, these nanoclusters can function as highly effective bioactive probes with considerable potential for fluorescent labeling and imaging of cancer cells.

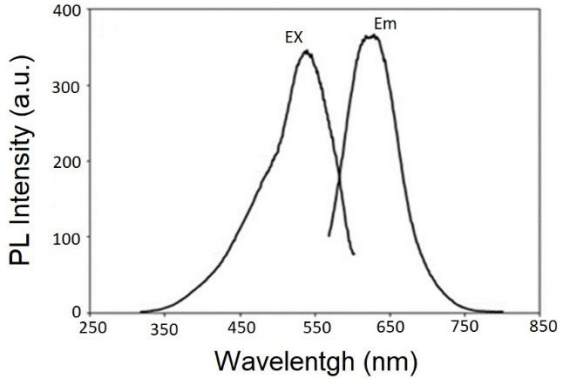


Figure 6. Excitation (Ex) and emission (Em) photoluminescence spectra of water-soluble BSA-stabilized copper nanoclusters (BSA–Cu NCs).

ICP spectroscopy can be used to quantitatively analyze most metallic and non-metallic elements. As you can see, the catalyst loading values obtained from direct mass-based calculations (1.26 mol%) and from ICP measurements (1.38 mol%) are very close, which confirms the reliability of the copper content determination and the consistency of the experimental procedure.

Thermogravimetric analysis (TGA) is a powerful technique used to investigate the thermal stability and compositional characteristics of materials, including catalysts, as a function of temperature and/or time by monitoring changes in sample weight during controlled heating [27]. In this study, TGA was employed to evaluate the thermal stability of the BSA ligand used for stabilizing the copper nanoclusters. As shown in the TGA curve (Figure 7), the thermal decomposition process proceeds through two distinct weight-loss stages. The first stage, occurring at temperatures below 150 °C, exhibits a noticeable weight loss of approximately 0.66 wt%, which is attributed to the removal of physically adsorbed water molecules acting as residual solvent. The second stage, observed over the temperature range of 150–450 °C, corresponds to the thermal degradation and combustion of the BSA ligand. The calculated weight loss in this region is approximately 20 wt%, which is equivalent to 6×10^{-5} mmol of BSA ligand. At temperatures above 450 °C, a residual mass of approximately 11 wt% remains, which is assigned to the copper content of the catalyst. This residue corresponds to 3×10^{-2} mmol of copper present in the nanocluster composition [5]. These results clearly confirm the successful incorporation of copper within the BSA-stabilized nanocluster framework and demonstrate the satisfactory thermal stability of the catalyst.

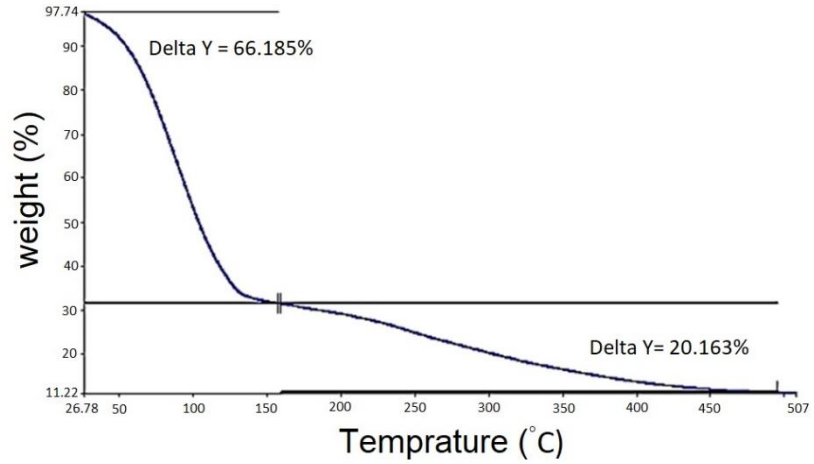


Figure 7. Thermogravimetric analysis (TGA) of copper nanoclusters

Catalytic Activity of BSA–Cu Nanoclusters in the Oxidation of Alcohols Using Molecular Oxygen/Air

To confirm that no oxidation occurs in the absence of a catalyst, the oxidation of benzyl alcohol (0.5 mmol) was carried out using molecular oxygen at 25°C under catalyst-free conditions. After 11 h, no detectable reaction progress was observed (Entry 1). Under otherwise identical conditions, the reaction was conducted in the presence of 1.38 mol% of BSA–Cu nanoclusters. Reaction evaluation after 1.5 h, in the presence of BSA–Cu NCs and isobutyraldehyde (8 mmol) as a cocatalyst, revealed quantitative conversion (100%). This result clearly shows how important the BSA–Cu NCs catalytic system is for activating molecular oxygen for the oxidation process (Entry 6). Under the same conditions but without isobutyraldehyde, the reaction only converted 30%, which shows how much the aldehyde cocatalyst helped (Entry 5). For comparison, the oxidation reaction was also done with 0.093 g (0.0069 mmol) of copper sulfate salt. After 11 hours, only about 5% conversion was seen (Entry 2). Similarly, when the reaction was done with BSA ligand alone as the catalyst, a similar low conversion was seen (Entry 3), showing that neither the copper salt nor the protein ligand alone works as a catalyst in these conditions. In a different experiment, the catalyst was made without hydrazine reduction. When this material was applied in the oxidation reaction, a conversion of 85% was achieved after 90 min; however, a noticeable decrease in selectivity was observed upon prolonged reaction time (Entry 4).

Table 1. Effect of Catalyst Nature, Ligand, Reducing Agent, and Cu^{2+} Source on the Oxidation of Benzyl Alcohol with Molecular Oxygen Catalyzed by BSA–Cu Nanoclusters[a].

Entry	Catalyst	Yield (%)
1	--- [(b)]	0
2	$CuSO_4$ [(c)]	<5
3	BSA [(d)]	<5
4	BSA-Cu^{2+} [(e)]	85
5	BSA-CuNCs [(f)]	30
6	BSA-CuNCs [(g)]	100

(a) Reaction conditions: benzyl alcohol (0.5 mmol), isobutyraldehyde (8 mmol), deionized water (3 mL), catalyst loading (1.38 mol% Cu, unless otherwise stated), O_2 (1 atm, 5 mL min^{-1}), 25 °C, reaction time 90 min. Product yields were determined by TLC analysis. (b) Reaction performed in the absence of catalyst. (c) Copper sulfate salt (0.093 g, 0.0069 mmol) used as catalyst. (d) BSA ligand alone (0.03 g) used as catalyst. (e) Catalyst prepared without hydrazine reduction. (f) Catalyst loading 1.38 mol% in the absence of isobutyraldehyde. (g) Catalyst loading 1.38 mol% (BSA–Cu NCs).

Optimal Reaction Conditions for the Catalytic Oxidation of Benzyl Alcohol

The Amount of BSA–Cu Nanocatalyst on the Oxidation of Benzyl Alcohol

To assess the influence of varying concentrations of BSA–Cu nanocatalyst on the oxidation of benzyl alcohol, distinct volumes of the aqueous BSA–Cu NCs solution were utilized while maintaining consistent reaction conditions. As illustrated in Figure 8, the oxidation of benzyl alcohol requires an amount of nanocatalyst corresponding to 1.38 mol% of Cu to achieve complete conversion. Increasing the amount of the nanocatalyst beyond this value does not result in any further improvement in the reaction yield. In contrast, reducing the amount of the nanocatalyst leads to a noticeable decrease in reaction progress.

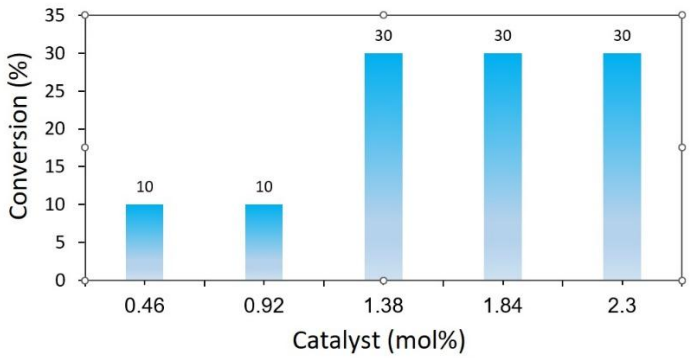


Figure 8. Effect of different amounts of BSA–Cu nanocatalyst on the catalytic oxidation of benzyl alcohol. The reaction was carried out using benzyl alcohol (0.05 mL, 0.5 mmol) under an O_2 atmosphere (1 atm, 5 mL min^{-1}) at 25 °C. Product formation was monitored by TLC after 90 minutes.

The Amount of Isobutyraldehyde on the Oxidation of Benzyl Alcohol

The aerobic oxidation of benzyl alcohol showed very little progress under the conditions used, so isobutyraldehyde was added as a co-catalyst to speed up the reaction. When the amount of isobutyraldehyde was increased, the reaction progressed much faster. The optimization study showed that the best amount of isobutyraldehyde to use was 8 mmol. Adding more isobutyraldehyde did not improve the reaction yield any further, and using less did not improve the oxidation efficiency. It is

important to note that no benzoic acid was formed under these reaction conditions, which shows that the reaction was very selective for the desired aldehyde product.

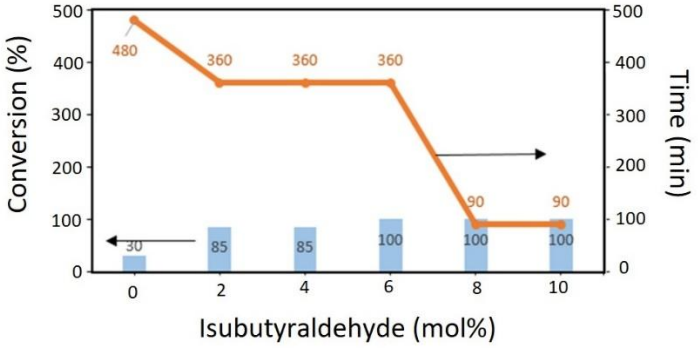


Figure 9. Effect of varying amounts of isobutyraldehyde on the oxidation of benzyl alcohol catalyzed by BSA–Cu nanoclusters (BSA–Cu NCs). The reaction was performed using benzyl alcohol (0.05 mL, 0.5 mmol) in the presence of BSA–Cu NCs (1.38 mol% Cu) under an O_2 atmosphere (1 atm, 5 mL min^{-1}) at 25 °C. Reaction progress was monitored by TLC.

Effect of Solvent Nature on the Oxidation of Benzyl Alcohol

We looked at how benzyl alcohol oxidized in different solvents, such as ethanol, methanol, water, acetone, and n-hexane, with 1.38 mol% of the BSA–Cu nanocatalyst. Figure 10 shows a summary of the results. Interestingly, high oxidation yields were achieved in both polar solvents, including water and methanol, and in the nonpolar solvent n-hexane. Water was chosen as the best reaction medium because it is good for the environment, not toxic, and long-lasting. This makes it especially good for green oxidation processes.

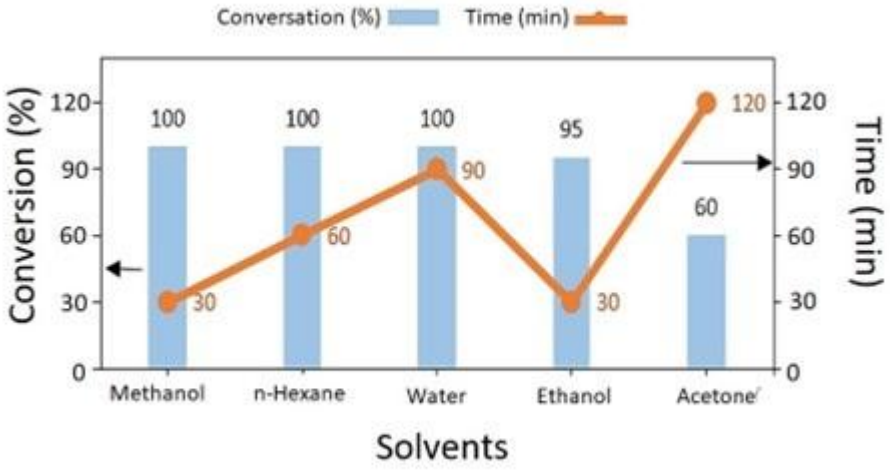


Figure 10. Effect of different solvents on the oxidation of benzyl alcohol catalyzed by BSA–Cu nanoclusters (BSA–Cu NCs). The reaction was carried out using benzyl alcohol (0.05 mL, 0.5 mmol) in the presence of BSA–Cu NCs (1.38 mol% Cu) and isobutyraldehyde (0.8 mL, 8 mmol) under an O_2 atmosphere (1 atm, 5 mL min^{-1}) at 25 °C. Reaction progress was monitored by TLC.

Effect of Water Amount on the Oxidation Reaction

To find out how much water was best for speeding up the oxidation reaction, different amounts of water were added to the reaction system. The results showed that 3 mL of water (32 mol%) was the

best amount, as it made the reaction go the fastest. When the amount of water was either lower or higher than this optimal value, the reaction rate and overall conversion changed in noticeable ways (Figure 11).

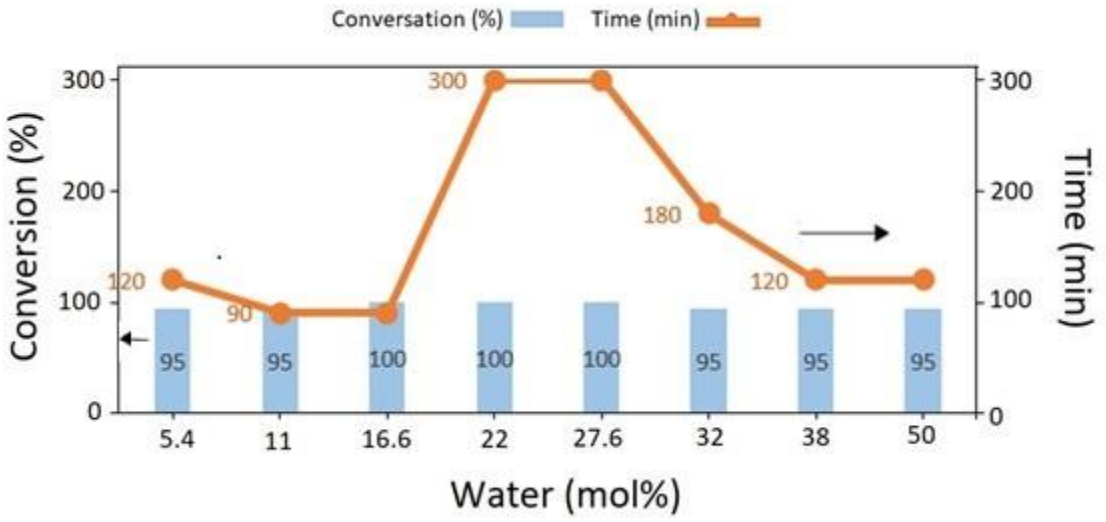


Figure 11. Effect of different amounts of water on the oxidation of benzyl alcohol catalyzed by BSA–Cu nanoclusters (BSA–Cu NCs). The reaction was carried out using benzyl alcohol (0.05 mL, 0.5 mmol) in the presence of BSA–Cu NCs (1.38 mol% Cu) and isobutyraldehyde (0.8 mL, 8 mmol) under an O_2 atmosphere (1 atm, 5 mL min^{-1}) at 25 °C. Reaction progress was monitored by TLC.

Effect of Temperature on the Oxidation Reaction

The effect of temperature on the oxidation reaction was studied in a systematic way. As shown in Figure 12, raising the temperature to 40 °C did not improve the reaction yield in any noticeable way. However, raising the temperature even more made the reaction less efficient. This is, because the BSA ligand breaks down and the copper nanoclusters start to aggregate at higher temperatures, which makes the catalytic activity worse. The reaction reached 100% conversion in a shorter time at room temperature, so room temperature(25°C) was chosen as the best condition for the next experiments.

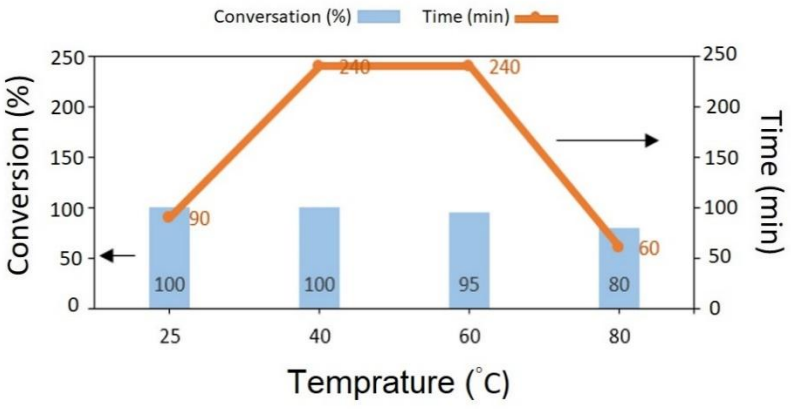


Figure 12. Effect of reaction temperature on the oxidation of benzyl alcohol catalyzed by BSA–Cu nanoclusters (BSA–Cu NCs). The reaction was carried out using benzyl alcohol (0.05 mL, 0.5 mmol) in the presence of BSA–Cu NCs (1.38 mol% Cu), isobutyraldehyde (0.8 mL, 8 mmol), and deionized water (3 mL) as the solvent, under an O_2 atmosphere (1 atm, 5 mL min^{-1}). Reaction progress was monitored by TLC.

Effect of Oxygen Flow Rate on the Oxidation Reaction

To find the best oxygen flow rate for the aerobic oxidation of alcohols in water, the reaction was studied with different O_2 flow rates and BSA–Cu nanoclusters (BSA–Cu NCs) in water as the solvent. All tests were done at 25 °C. The results showed that an oxygen flow rate of 5 mL min^{-1} gave the best reaction efficiency. Increasing the oxygen flow rate above this level did not improve the reaction and may have caused some of the reactants and/or products to be stripped from the reaction medium. On the other hand, lowering the oxygen flow rate made it hard for the reaction to happen. Therefore, an oxygen flow rate of 5 mL min^{-1} was chosen as the best condition for the next oxidation reactions.

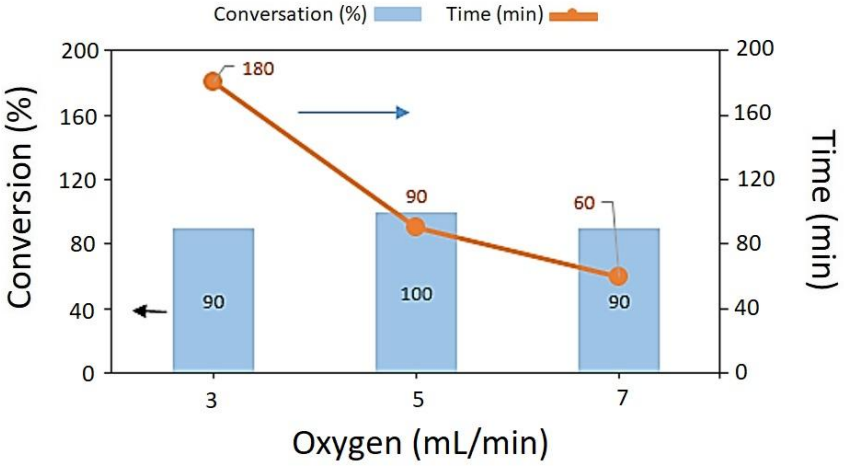


Figure 13. Effect of oxygen flow rate on the oxidation of benzyl alcohol catalyzed by BSA–Cu nanoclusters (BSA–Cu NCs). The reaction was carried out using benzyl alcohol (0.05 mL, 0.5 mmol) in the presence of BSA–Cu NCs (1.38 mol% Cu), isobutyraldehyde (0.8 mL, 8 mmol), and deionized water (3 mL) as the solvent. The oxidation was performed under an O_2 atmosphere (1 atm) at different flow rates, and the reaction progress was monitored by TLC.

Measurement of Oxygen Consumption during the Reaction

The consumption of oxygen in the reaction medium was investigated to gain further insight into the oxidation process. As shown in Figure 14, the amount of oxygen uptake by benzyl alcohol was compared in the presence of copper sulfate salt and water-soluble copper nanoclusters (BSA–Cu NCs). This clear difference shows that the nanocluster catalyst makes it easier for molecular oxygen to be activated and moved than the homogeneous copper salt. The increased oxygen consumption is consistent with the greater catalytic activity and selectivity seen in BSA–Cu NCs. This supports the idea that the nanocluster structure and protein stabilization play a role in promoting aerobic oxidation in mild and environmentally friendly conditions.

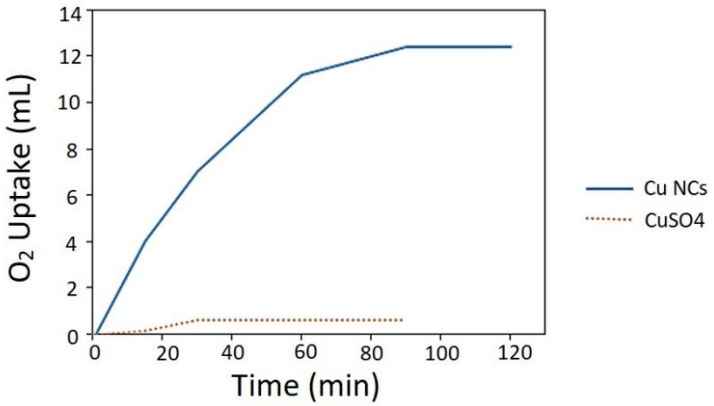


Figure 14. Comparison of oxygen absorption by benzyl alcohol in the presence of copper sulfate salt ($CuSO_4$) and water-soluble copper nanoclusters (BSA–Cu NCs) in aqueous medium at 25 °C.

Comparison of the Catalytic Activity of Cu-NCs Prepared at Different pH Values

The BSA ligand adopts different conformations at different pH values, leading to variations in the metal–ligand interactions and, consequently, in the structure and catalytic performance of the resulting copper nanoclusters. To evaluate these effects, the aerobic oxidation of alcohols in aqueous solution was investigated using Cu-NCs catalysts, synthesized at various pH levels (Figure 15). While the catalyst synthesized at pH 9 achieved 95% conversion within 30 minutes, reaching a plateau after 11 hours with no further improvement, the catalysts prepared at pH 6 and pH 12 both reached complete conversion (100%) within only 90 minutes. Although the catalysts prepared at pH 6 and pH 12 exhibited identical yields (100%) after 90 minutes; We selected pH 12 for the catalytic reaction because the selectivity of this reaction was low at pH 6.

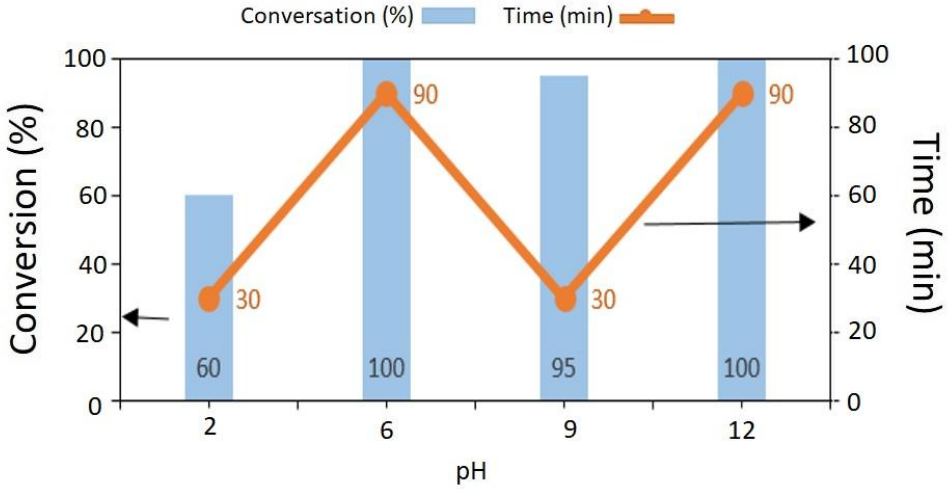


Figure 15. Comparison of the catalytic activity of Cu-NCs synthesized at different pH values in the aerobic oxidation of benzyl alcohol. The reaction was carried out using benzyl alcohol (0.05 mL, 0.5 mmol), Cu-NC catalyst (1.38 mol%), isobutyraldehyde (0.8 mL, 8 mmol), and deionized water (3 mL) under an O_2 atmosphere (1 atm, flow rate: 5 mL min^{-1}) at 25 °C. The reaction progress and conversion were determined by TLC analysis.

Investigation of Stability Aqueous Cu-NCs Catalyst Solutions prepared at Different pH Values by UV–Vis Spectroscopy

To assess the stability of aqueous solutions of Cu–NC catalysts synthesized at varying pH levels, UV–Vis absorption spectra were obtained. Figure 16 shows that the catalysts have their usual absorption bands at about 280 nm and 230 nm for all of the pH levels that were tested. The band at 280 nm is due to the π→π* transitions of the BSA ligand, and the band at 230 nm is related to ligand-to-metal charge transfer (LMCT).

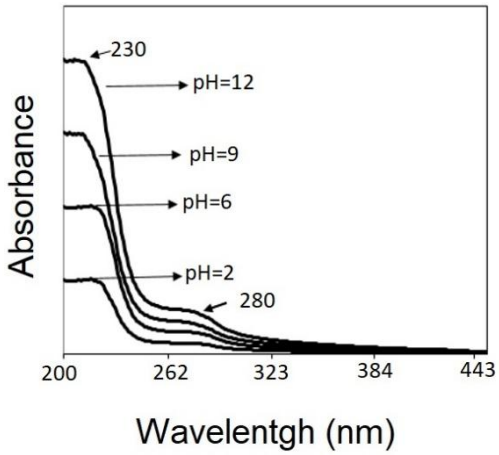


Figure 16. UV–Vis absorption spectra of BSA-stabilized copper nanoclusters (BSA–Cu NCs) synthesized at different pH values.

Aerobic Oxidation of Various Alcohols Catalyzed by BSA–Cu NCs

After optimization of the reaction conditions, the efficiency and generality of this newly developed catalytic system were evaluated for the aerobic oxidation of a variety of alcohols using air or molecular oxygen as the oxidant. The results are summarized in Table 2.

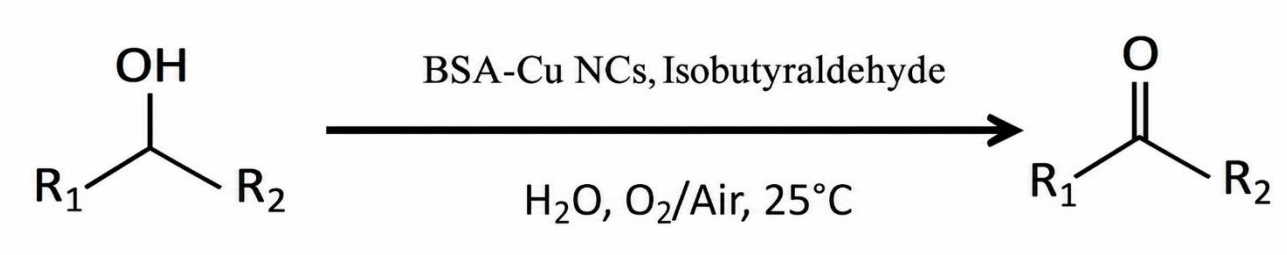
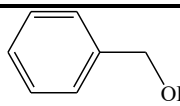
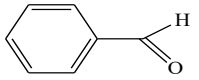
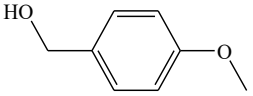
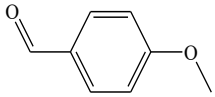
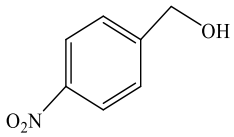
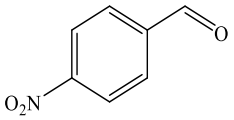
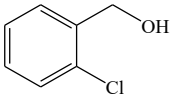
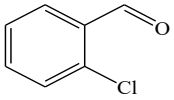
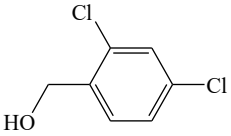
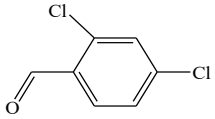
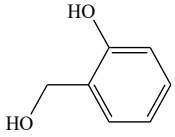
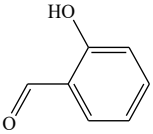
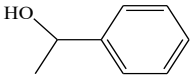
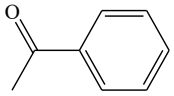
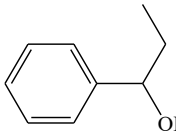
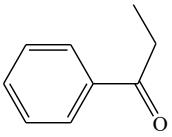
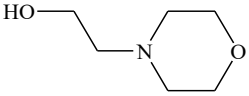
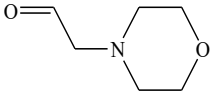
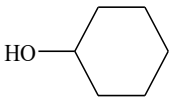
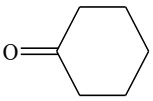
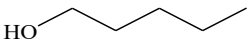
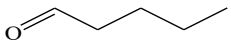
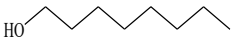
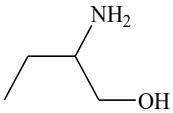
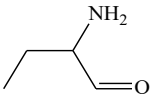
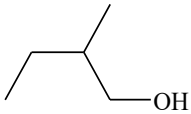
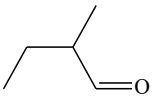
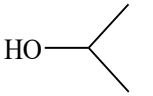
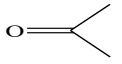


Figure 17. General reaction scheme for the oxidation of alcohols to carbonyl compounds catalyzed by BSA-Cu NCs.

Benzyl alcohol and its derivatives were selectively oxidized to the corresponding carbonyl compounds without overoxidation using either molecular oxygen or air as the terminal oxidant. Both electron-donating and electron-withdrawing substituents were well tolerated under the optimized reaction conditions, as shown in Table 2, demonstrating the wide range of applications of the BSA–Cu NC catalytic system. Alcohols with electron-withdrawing groups, like 4-nitrobenzyl alcohol (entry 3), showed lower oxidation rates than secondary benzylic alcohols, such as 1-phenyl-1-propanol (entry 8) and benzyl alcohol (entry 1). When air was used as the oxidant, 1-phenyl-1-propanol (entry 8) was also oxidized more quickly than electron-deficient substrates, showing a similar pattern. These findings unequivocally show that the aerobic oxidation process is significantly influenced by electronic effects. Remarkably, the BSA–Cu NCs catalyst also showed excellent aliphatic alcohol efficiency. While 2-methyl-1-butanol (entry 14) and cyclohexanol (entry 10) demonstrated relatively higher reaction rates when air was used as the oxidant, 1-octanol (entry 12) was oxidized efficiently in the presence of molecular oxygen. Aliphatic substrates—1-octanol under O_2 and 2-methyl-1-butanol and cyclohexanol under air—were oxidized more quickly than their aromatic counterparts, according to a comparison of aromatic and aliphatic alcohols. It's interesting to note that steric effects seem to have little effect on regulating the oxidation process in both oxygen and air. The similar reaction rates of 4-nitrobenzyl alcohol (para-substituted, entry 3) and 2-hydroxybenzyl alcohol (ortho-substituted, entry 6) demonstrate that the positional effects of substituents on the aromatic ring have little effect on the catalytic performance. Similarly, benzyl alcohol derivatives bearing 2,4-dichloro (entry 5) and 2-chloro (entry 4) substituents exhibited nearly identical reactivities. Furthermore, under otherwise identical conditions and regardless of the oxidant employed (O_2 or air), the degree of the alcohol (primary vs. secondary) does not appear to strongly govern product formation. In fact, certain secondary alcohols, such as 1-phenyl-1-propanol (entry 8), displayed higher reactivity than benzyl alcohol itself (entry 1), underscoring the unique reactivity profile of the BSA–Cu NCs catalyst.

Table 2. Aerobic Oxidation of Various Alcohols Catalyzed by BSA–Cu NCs[a]

Entry	Reactant	Product	Time(h)		Conversion (%)	
			Air	O_2	Air	O_2

1			1.5	1.5	100	100
2			2	2	100	90
3			2	2	40	40
4			0.5	3	85	80
5			1.5	1.5	80	70
6			0.5	2.5	80	60
7			0.5	2	90	60
8			0.75	1.5	100	100
9			1.5	1	100	100
10			0.5	1.5	100	100
11			4	0.5	85	60
12			1	0.5	100	100
13			1	0.5	100	60
14			0.5	2	100	95
15			5	2	100	100

[a] Reaction conditions: alcohol (0.5 mmol), BSA–Cu NC catalyst (1.38 mol% Cu), isobutyraldehyde (8 mmol), deionized water (3 mL), under an O_2 atmosphere (1 atm, flow rate: 5 mL min^{-1}) or air, at 25 °C for. Product yields were determined by TLC. In all cases, the selectivity toward the desired carbonyl products was higher than 99%.

Product Identification by ^{1}H NMR Spectroscopy

The structures of selected oxidation products were corroborated through the comparison of their ^{1}H NMR spectra with those documented in the literature. For instance, the ^{1}H NMR spectrum of propiophenone (entry 8) displayed distinctive resonances that aligned with its molecular structure.

Specifically, two multiplets in the ranges of δ 7.69–7.77 ppm (integrating for 2 H) and δ 7.26–7.45 ppm (integrating for 3 H) were identified as the aromatic protons of the phenyl ring. Additionally, a multiplet at δ 4.54–4.66 ppm, integrating for 2 H, was attributed to the methylene (CH_2) protons of the ethyl group. A triplet at δ 1.14 ppm, integrating for 3 H, was assigned to the methyl (CH_3) protons of the ethyl substituent (Figure S1).

The structures of certain products were elucidated by comparing their ^{1}H NMR spectra with previously documented data. For example, the ^{1}H NMR spectrum of 2-aminobutanal (entry 13) showed signals that were typical for its molecular structure. The aldehydic proton (–CHO) was given a unique resonance at δ 9.80 ppm that integrated for 1 H. A multiplet seen between δ 4.26 and 4.28 ppm with an integration of 1 H was thought to be the methine (CH) proton next to the amino group. In addition, a singlet at δ 2.84 ppm, integrating for 2 H, was assigned to the amino ($–NH_2$) protons, appearing as a relatively broad signal due to proton exchange. Additionally, a multiplet within the range of δ 1.76–1.88 ppm, integrating for 2 H, was assigned to the methylene (CH_2) protons, while a triplet at δ 1.26 ppm, integrating for 3 H, corresponded to the methyl (CH_3) group. These spectral characteristics align well with documented ^{1}H NMR data for 2-aminobutanal, validating its successful synthesis (Figure S2).

Catalyst Reusability and Stability

We tested how well the BSA–Cu NCs catalyst could be recovered and reused by using it in the aerobic oxidation of alcohols under the best reaction conditions. After the first catalytic run was finished, 5 mL of diethyl ether was added to the reaction mixture, and the mixture was stirred gently for 5 minutes. It was easy to extract the products because diethyl ether easily dissolves organic products and leftover organic species. After phase separation, the aqueous phase containing the BSA–Cu NCs catalyst was easily isolated. We did this extraction process three times to make sure that all of the organic parts were gone. The aqueous catalyst solution that had been recovered was then heated indirectly at 35 °C for 5 minutes to get rid of any remaining diethyl ether. After the first run, the recovered catalyst was used again for a second catalytic cycle under the same conditions, but without adding new isobutyraldehyde. After the reaction was over, the catalyst was separated again using the same extraction method. The catalyst that had been recovered was then used in a third oxidation cycle. In this run, in order to maintain catalytic activity, 0.8 mmol of isobutyraldehyde was added at the beginning of the reaction, similar to the first cycle. The catalyst was recovered after the third run using the same method as before. Figure 18 shows the catalytic performance of the BSA–Cu NCs over three cycles in a row. This clearly shows that this homogeneous catalyst can be used again and again and is stable in use. The extraction efficiency was also tested with different organic solvents, such as acetone, ethyl acetate, dichloromethane, and diethyl ether. Diethyl ether was the best extraction solvent out of these because it made phase separation cleaner and made it easier to get the aqueous catalyst phase back. For this reason, it was used in all of the recycling tests.

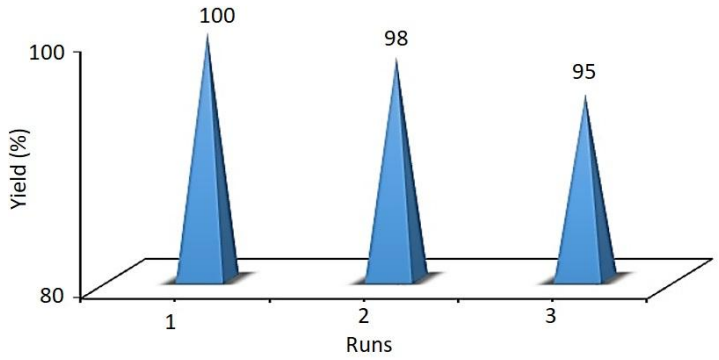


Figure 18. Evaluation of the reusability of BSA–Cu NCs catalyst in the aerobic oxidation of benzyl alcohol using air/O_2. The reaction was carried out in the presence of 0.05 mL (0.5 mmol) benzyl alcohol, 1.38 mol% BSA–Cu NCs catalyst, 0.8 mL (8 mmol) isobutyraldehyde as a co-catalyst, and 3 mL of water as the solvent, under 1 atm oxygen pressure with an O_2 flow rate of 5 mL min^{-1}, at 25 °C. The reaction progress and oxidation yield were determined after 90 min using TLC.

Post-reaction characterizations of the catalyst including FT-IR spectra, UV-Vis spectra and, TEM image after O_2-mediated oxidation of benzyl alcohol Figures(S3-S5) and after aerobic oxidation of benzyl alcohol Figures(S6-S8) were confirmed the stability of the catalyst after both reactions. (supporting information)

Mechanistic Evidence and Discussion

To explain how oxidation happens when air or molecular oxygen (O_2) is present as the oxidant, we took UV–Vis spectra of the reaction mixture at different times (1, 5, 10, 15, 30, 45, 75, and 90 minutes). The electronic absorption spectra of the copper nanoclusters didn't change much during the oxidation process, which means that the electronic structure of the BSA–Cu NCs stays the same throughout the reaction. Based on these results, we can rule out the formation of η^2-peroxo, superoxo, or μ^2-peroxo copper–oxygen species during the aerobic oxidation process.

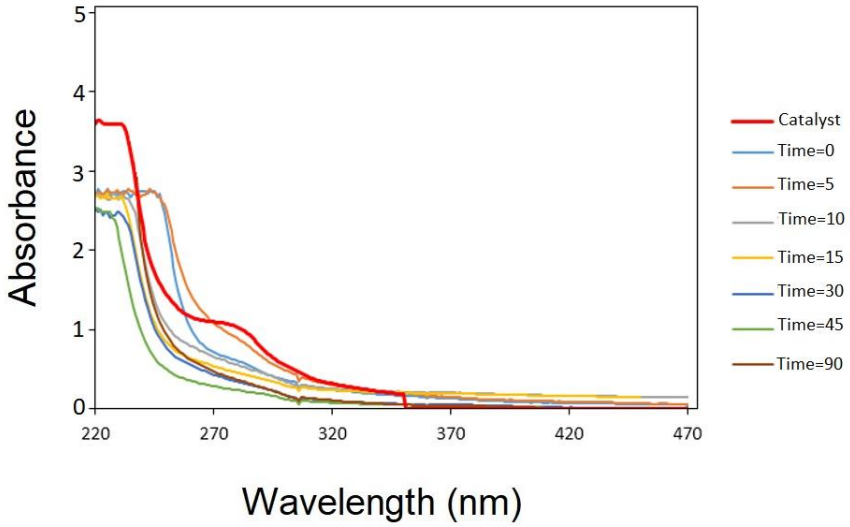


Figure 19. UV–Vis spectral monitoring during the oxidation of benzyl alcohol with air/O_2 in the presence of BSA–Cu nanoclusters (BSA–Cu NCs).

Furthermore, 1.38 mol% of the nanocatalyst was added to a reaction mixture containing 0.5 mmol of benzyl alcohol, 1.5 mL of deionized water, 8 mmol of isobutyraldehyde, and 1 mmol of the radical scavenger 2-tert-butyl-4-methylphenol (BHT), and the reaction mixture was stirred at 25 °C. Under these conditions, a significant suppression of the reaction progress was observed. In addition, the reaction was also performed in the presence of 1 mmol of another radical scavenger, diphenylamine,

which led to a similar inhibitory effect. Moreover, the reaction was repeated under identical conditions using 5-fold and 10-fold excesses (relative to benzyl alcohol) of both radical scavengers, 2-tert-butyl-4-methylphenol and diphenylamine, and comparable results were obtained. These observations clearly indicate that the aerobic oxidation of benzyl alcohol in the presence of BSA–Cu nanoclusters proceed via a radical mechanism when air or molecular oxygen (O_2) is used as the oxidant.

The proposed mechanism for the oxidation of benzyl alcohol with molecular oxygen in the presence of copper nanoclusters in an aqueous medium is depicted in Figure 20, based on the preceding observations. X-ray photoelectron spectroscopy (XPS) showed that the oxidation states of copper in the BSA–Cu nanoclusters were Cu(0) and Cu(II). Previous reports indicate that the catalytic cycle is initiated by Cu(II) species. The presence of metallic copper (Cu^0) is essential for increasing catalytic activity and achieving 100% selectivity, as shown by the results in Table 1.

In the proposed mechanism, benzyl alcohol ($PhCH_2OH$) is initially coordinated to the Cu–BSA complex, and water is generated as a by-product during this step (Figure 20, step a). It is clear that removing β-hydrogen from the coordinated benzyl alcohol creates the corresponding aldehyde, benzaldehyde (Figure 20, step b). The most important step in this catalytic system is the activation of the benzylic hydrogen by isobutyraldehyde, which acts as a co-catalyst (Figure 20, step c). At the same time, the corresponding hydroxy-isobutyraldehyde intermediate is created, which is then re-oxidized to isobutyraldehyde by molecular dioxygen, which regenerates the co-catalyst and keeps the catalytic cycle going. The Cu(I)–BSA nanocluster species that form during the reaction are then re-oxidized to Cu(II) by molecular oxygen (O_2) (Figure 20, step d). This redox transformation is a well-known and typical feature of copper-based catalytic systems that ensures the active Cu(II) species are regenerated and the catalytic cycle continues[46], [38][39].

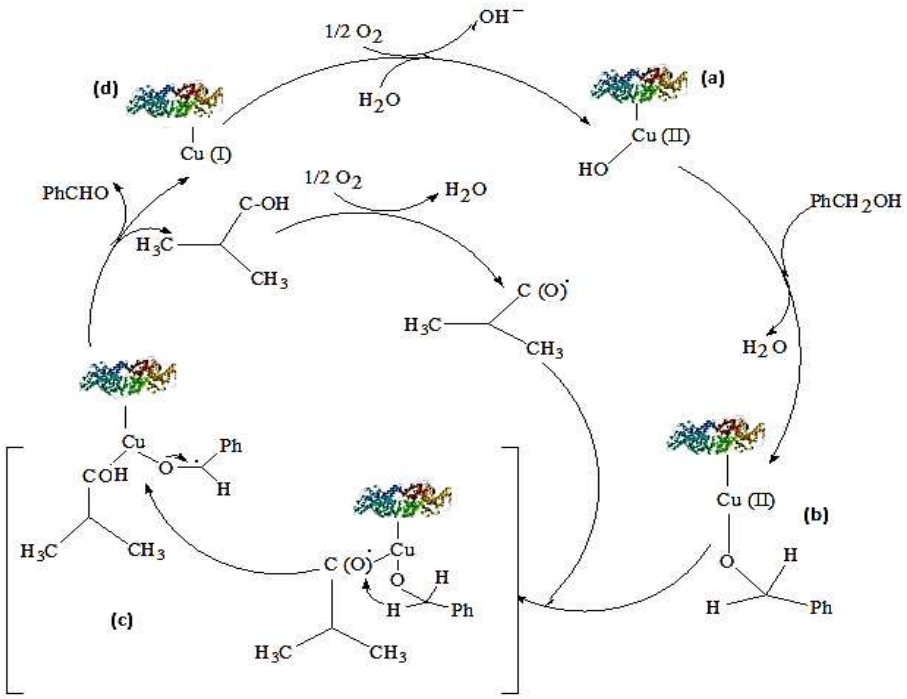
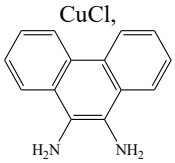
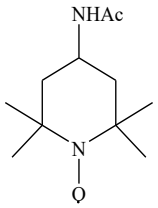
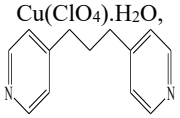


Figure 20. Proposed mechanism for the catalytic oxidation of benzyl alcohol using air or molecular oxygen (O_2) in the presence of the Cu–BSA nanocluster system in an aqueous medium.

Comparison of alcohol oxidation catalyzed by copper catalysts under aerobic conditions

Table 3 provides a comparative overview of representative copper-catalyzed aerobic oxidation systems reported for the conversion of alcohols to the corresponding carbonyl compounds. The comparison clearly highlights the distinct advantages of the present BSA–Cu nanocluster catalytic system over previously reported copper-based methodologies.

Table 3. Comparative study of copper-catalyzed aerobic oxidation of alcohols

Entry	Substrates	Co-oxidant	Ligand/Complex	Add.	Reaction Condition	Yields (%)
1	Banzylic	----------	$CuCl_2$	$CsCO_3$	Toluene O_2, 12 h	72-94, [40]
2	Banzylic 1° Aliphatic	----------	CuCl, 	NaOH	H_2O, 100 °C, 10 atm, O_2, 3 h	57-99, [41]
3	Banzylic Allylic 1° Aliphatic 2° Aliphatic	Graghite electrode	2,2′-bisquinoline polymer	$LiClO_4$, Bu_4BF_4	rt	85-94, [42]
4	Banzylic	----------	CuCl, phen	K_2CO_3	Benzene, reflux, O_2	83-93, [43]
5	Banzylic	----------	CuCl, phen	K_2CO_3	DMF/Benzene, reflux, O_2, 2 h	65-86, [44]
6	Banzylic Allylic		$Cu(ClO_4).H_2O$, 	DABCO	DMSO, rt, O_2, 2 h	71-98, [45]
7	Banzylic Allylic 1° Aliphatic	Built into ligand	$CuBr_2$, Me_2S, bipy	NMI or DBU	MeCN, rt, 1-5 h, 1 atm O_2	55-94, [46]
8	Banzylic Allylic 1° Aliphatic	TEMPO	$Cu(MeCN)_4X$ X=OTF^-, BF^-, PF_6^- bipy	NMI	MeCN, air, O_2, rt	79-98, [25]
9	Banzylic Allylic 1° Aliphatic	TEMPO	$CuBr_2$, bipy	t-BuOK	MeCN/H_2O,25 ◦C, air, 2.5-5 h	91-100, [47]
10	Banzylic	resin-supported TEMPO	resin-supported CuCl-Phen	----------	DMF, air, rt, 24 h	100, [48]
11	Banzylic Allylic	TEMPO	HKUST-1	Na_2CO_3	CH_3CN, O_2, 75 ◦C, 22 h	3-89, [49]
12	Banzylic	TEMPO	Cu-MOF-2	Na_2CO_3	CH_3CN, O_2, 75 ◦C, 16 h	99, [50]
13	Benzylic	TEMPO	Cu(I/II)-AmP-CPG (5mol% of Cu)	----------	O_2, 50 ◦C, 5.5 h	97[a], [51]
14	Benzylic	----------	Cu NP zeolite	K_2CO_3	Air, 60 ◦C, 24 h	100, [52]
Our work	**Banzylic**	**Isobutyraldehyde**	**BSA-Cu NCs**	**----------**	**H_2O, rt, 1 bar O_2, 1.5 h**	**100**

a) Yield of purified products

Most literature-reported copper systems (Entries 1–14) rely on copper salts or complexes, typically in combination with external ligands (bipyridine, phenanthroline), bases (Cs_2CO_3, K_2CO_3, t-BuOK, NaOH), or radical mediators such as TEMPO. Although these systems often afford moderate to excellent yields (55–100%), they generally require harsh or less sustainable conditions, including elevated temperatures, organic solvents (toluene, DMF, DMSO, MeCN), high oxygen pressure, long reaction times, or high catalyst/additive loadings. In contrast, the present work demonstrates that BSA–Cu nanoclusters efficiently catalyze the aerobic oxidation of benzylic alcohols under remarkably mild and environmentally benign conditions. The reaction proceeds in pure water, at room temperature, under 1 bar O_2, and without the need for external ligands, bases, or nitroxyl radicals. Notably, complete conversion (100%) is achieved within 1.5 h, which compares favorably with many TEMPO-assisted copper systems that require longer reaction times and higher catalyst loadings. A particularly important distinction is the use of isobutyraldehyde as a co-oxidant, which replaces traditional nitroxyl radicals and bases. Control experiments confirm that isobutyraldehyde plays a critical role in promoting the oxidation process, enabling high activity while maintaining excellent selectivity toward aldehydes and ketones, with no detectable over-oxidation to carboxylic acids. This feature represents a significant mechanistic and practical advancement over classical Cu/TEMPO/O_2 systems. Furthermore, the nanocluster nature of the catalyst, stabilized by a biogenic BSA scaffold, provides a unique microenvironment that facilitates Cu(0)/Cu(II) redox cycling while maintaining structural stability under aerobic conditions. This dual-valence copper state, absent in most conventional homogeneous systems, is believed to be responsible for the enhanced catalytic efficiency and selectivity observed in this work. Overall, the data summarized in Table 3 clearly demonstrate that the BSA–Cu nanocluster system outperforms many previously reported copper-based aerobic oxidation catalysts by combining high efficiency, operational simplicity, aqueous media compatibility, and green chemistry credentials. These features position the present catalytic system as a promising and sustainable alternative for aerobic alcohol oxidation, with potential relevance to both academic research and practical synthetic applications.

Conclusion

BSA-stabilized copper nanoclusters (BSA–Cu NCs) were successfully synthesized and comprehensively characterized, confirming their ultrasmall size, structural stability, and strong photoluminescence originating from ligand-to-metal charge transfer. The nanoclusters exhibited outstanding catalytic activity in the selective aerobic oxidation of various alcohols to their corresponding carbonyl compounds under mild aqueous conditions (25 °C, air or O_2, >99 % selectivity). Optimization studies demonstrated that catalyst loading, isobutyraldehyde cocatalyst, and oxygen flow critically influence the catalytic efficiency, while water served as a green and effective solvent. Spectroscopic and microscopic analyses confirmed that the BSA–Cu NCs preserve their structural integrity and electronic stability during catalysis, with minimal ligand dissociation. The system could be reused for at least three consecutive cycles with negligible loss of activity. Compared to other copper-based systems, the BSA–Cu NC catalyst offers superior efficiency, operational stability, and environmental compatibility, establishing it as a highly efficient bio-derived platform for sustainable aerobic oxidation reactions. The oxidation conversion observed under air was marginally higher than that obtained under pure O_2, which may be attributed to the enhanced stability of the catalyst complex in an air atmosphere relative to a pure oxygen environment.

References

[1] C. Burda, X. Chen, R. Narayanan, and M. A. El-Sayed, “Chemistry and properties of nanocrystals of different shapes,” *Chem. Rev.*, vol. 105, no. 4, pp. 1025–1102, 2005, doi: 10.1021/cr030063a.

[2] J. Lalonde and A. Margolin, *Enzyme Catalysis in Organic Synthesis: A Comprehensive Handbook, Second Edition*. Wiley-VCH, 2008.

[3] J. Kim, “Nanobiocatalysis and its potential applications,” *Top. Catal.*, vol. 55, no. 16–18, pp. 1055–1056, 2012, doi: 10.1007/s11244-012-9907-y.

[4] C. Wang, C. Wang, L. Xu, H. Cheng, Q. Lin, and C. Zhang, “Protein-directed synthesis of pH-responsive red fluorescent copper nanoclusters and their applications in cellular imaging and catalysis,” *Nanoscale*, vol. 6, no. 3, pp. 1775–1781, 2014, doi: 10.1039/c3nr04835g.

[5] L. F. T. de Resende *et al.*, “Revisiting the conformational transition model for the pH dependence of BSA structure using photoluminescence, circular dichroism, and ellipsometric Raman spectroscopy,” *Int. J. Biol. Macromol.*, vol. 259, p. 129142, 2024, doi: 10.1016/j.ijbiomac.2023.129142.

[6] S. I. Tanaka, J. Miyazaki, D. K. Tiwari, T. Jin, and Y. Inouye, “Fluorescent platinum nanoclusters: Synthesis, purification, characterization, and application to bioimaging,” *Angew. Chemie - Int. Ed.*, vol. 50, no. 2, pp. 431–435, 2011, doi: 10.1002/anie.201004907.

[7] Y. Cui *et al.*, “Serial silver clusters biomineralized by one peptide,” *ACS Nano*, vol. 5, no. 11, pp. 8684–8689, 2011, doi: 10.1021/nn202566n.

[8] R. Jin, Y. Zhu, and H. Qian, “Catalysis opportunities of atomically precise gold nanoparticles,” *ACS Natl. Meet. B. Abstr.*, vol. 21, no. 19, pp. 6793–6799, 2011.

[9] Z. Huang, F. Cui, H. Kang, J. Chen, X. Zhang, and C. Xia, “Highly dispersed silica-supported copper nanoparticles prepared by precipitation-gel method: A simple but efficient and stable catalyst for glycerol hydrogenolysis,” *Chem. Mater.*, vol. 20, no. 15, pp. 5090–5099, 2008, doi: 10.1021/cm8006233.

[10] Y. Zhu, H. Qian, M. Zhu, and R. Jin, “Thiolate-protected Aun nanoclusters as catalysts for selective oxidation and hydrogenation processes,” *Adv. Mater.*, vol. 22, no. 17, pp. 1915–1920, 2010, doi: 10.1002/adma.200903934.

[11] C. J. Li and T. H. Chan, *Comprehensive Organic Reactions in Aqueous Media: Second Edition*. John Wiley & Sons, 2006. doi: 10.1002/9780470131442.

[12] F. Yang *et al.*, “CO oxidation on inverse CeO x/Cu(111) catalysts: High catalytic activity and ceria-promoted dissociation of O 2,” *ACS Natl. Meet. B. Abstr.*, vol. 133, no. 10, pp. 3444–3451, 2011.

[13] T. Ke *et al.*, “Microfluidic synthesis of monodisperse cu nanoparticles in aqueous solution,” *J. Nanosci. Nanotechnol.*, vol. 11, no. 6, pp. 5154–5158, 2011, doi: 10.1166/jnn.2011.4160.

[14] G. H. Chan, J. Zhao, E. M. Hicks, G. C. Schatz, and R. P. Van Duyne, “Plasmonic properties of copper nanoparticles fabricated by nanosphere lithography,” *Nano Lett.*, vol. 7, no. 7, pp. 1947–1952, 2007, doi: 10.1021/nl070648a.

[15] N. A. Dhas, C. P. Raj, and A. Gedanken, “Synthesis, Characterization, and Properties of Metallic Copper Nanoparticles,” *Chem. Mater.*, vol. 10, no. 5, pp. 1446–1452, 1998, doi: 10.1021/cm9708269.

[16] E. A. Karakhanov *et al.*, “Copper nanoparticles as active catalysts in hydroxylation of phenol by hydrogen peroxide,” *Appl. Catal. A Gen.*, vol. 385, no. 1–2, pp. 62–72, 2010, doi: 10.1016/j.apcata.2010.06.042.

[17] C. Liu, S. Tanga, and A. Lei, “Oxidant controlled pd-catalysed selective oxidation of primary alcohols,” *Chem. Commun.*, vol. 49, no. 13, pp. 1324–1326, 2013, doi: 10.1039/c2cc38086b.

[18] J. U. Ahmad, “Copper Catalysts for Alcohol Oxidation,” 2012, *the Faculty of Science of the University of Helsinki Yliopistonkatu, Helsinki*.

[19] M. Contel, C. Izuel, M. Laguna, P. R. Villuendas, P. J. Alonso, and R. H. Fish, “Fluorous biphasic catalysis: Synthesis and characterization of copper(I) and copper(II) fluoroponytailed 1,4,7-Rf-TACN and 2,2′-R f-bipyridine complexes - Their catalytic activity in the oxidation of hydrocarbons, olefins, and alcohols, including mechanis,” *Chem. - A Eur. J.*, vol. 9, no. 17, pp. 4168–4178, 2003, doi: 10.1002/chem.200304771.

[20] I. E. Markó, M. Tsukazaki, P. R. Giles, S. M. Brown, and C. J. Urch, "Anaerobic Copper-Catalyzed Oxidation of Alcohols to Aldehydes and Ketones," *Angew. Chemie (International Ed. English)*, vol. 36, no. 20, pp. 2208–2210, 1997, doi: 10.1002/anie.199722081.
[21] P. Gamez, I. W. C. E. Arends, J. Reedijk, and R. A. Sheldon, "Copper(ii)-catalysed aerobic oxidation of primary alcohols to aldehydes," *Chem. Commun.*, vol. 3, no. 19, pp. 2414–2415, 2003, doi: 10.1039/b308668b.
[22] B. Betzemeier, M. Cavazzini, S. Quici, and P. Knochel, "Copper-catalyzed aerobic oxidation of alcohols under fluorous biphasic conditions," *Tetrahedron Lett.*, vol. 41, no. 22, pp. 4343–4346, 2000, doi: 10.1016/S0040-4039(00)00620-1.
[23] M. F. Semmelhack, C. R. Schmid, D. A. Cortés, and C. S. Chou, "Oxidation of Alcohols to Aldehydes with Oxygen and Cupric Ion, Mediated by Nitrosonium Ion," *J. Am. Chem. Soc.*, vol. 106, no. 11, pp. 3374–3376, 1984, doi: 10.1021/ja00323a064.
[24] C. J. Gartshore and D. W. Lupton, "Readily accessible oxazolidine nitroxyl radicals: Bifunctional cocatalysts for simplified copper based aerobic oxidation," *Adv. Synth. Catal.*, vol. 352, no. 18, pp. 3321–3328, 2010, doi: 10.1002/adsc.201000627.
[25] J. M. Hoover and S. S. Stahl, "Highly practical copper(I)/TEMPO catalyst system for chemoselective aerobic oxidation of primary alcohols," *J. Am. Chem. Soc.*, vol. 133, no. 42, pp. 16901–16910, 2011, doi: 10.1021/ja206230h.
[26] D. Cui, P. Huang, Z. Li, and H. Hu, "Synthesis and characterization of bovine serum albumin-conjugated copper sulfide nanocomposites," *J. Nanomater.*, vol. 2010, no. 1, p. 641545, 2010, doi: 10.1155/2010/641545.
[27] G. Mishra, D. Singh, P. K. Yadawa, S. K. Verma, and R. R. Yadav, "Study of copper/palladium nanoclusters using acoustic particle sizer: The preparation and non-destructive characterisation of bimetallic nanoclusters," *Platin. Met. Rev.*, vol. 57, no. 3, pp. 186–191, 2013, doi: 10.1595/147106713X667632.
[28] M. R. Mauk, F. I. Rosell, B. Lelj-Garolla, G. R. Moore, and A. G. Mauk, "Metal ion binding to human hemopexin," *Biochemistry*, vol. 44, no. 6, pp. 1864–1871, 2005, doi: 10.1021/bi0481747.
[29] S. F. Sun and N. O. del Rosario, "The Size and Shape of Bovine Serum Albumin in Acidic Water-Dioxane Mixtures," *J. Am. Chem. Soc.*, vol. 92, no. 7, pp. 1837–1839, 1970, doi: 10.1021/ja00710a008.
[30] H. Chen, L. Lin, H. Li, J. Li, and J. M. Lin, "Aggregation-induced structure transition of protein-stabilized zinc/copper nanoclusters for amplified chemiluminescence," *ACS Nano*, vol. 9, no. 2, pp. 2173–2183, 2015, doi: 10.1021/acsnano.5b00141.
[31] L. Zhang and E. Wang, "Metal nanoclusters: New fluorescent probes for sensors and bioimaging," *Nano Today*, vol. 9, no. 1, pp. 132–157, 2014, doi: 10.1016/j.nantod.2014.02.010.
[32] X. Yuan *et al.*, "Synthesis of highly fluorescent metal (Ag, Au, Pt, and Cu) nanoclusters by electrostatically induced reversible phase transfer," *ACS Nano*, vol. 5, no. 11, pp. 8800–8808, 2011, doi: 10.1021/nn202860s.
[33] C. Vázquez-Vázquez, M. Bañobre-López, A. Mitra, M. A. López-Quintela, and J. Rivas, "Synthesis of small atomic copper clusters in microemulsions," *Langmuir*, vol. 25, no. 14, pp. 8208–8216, 2009, doi: 10.1021/la900100w.
[34] H. Qian, M. Zhu, Z. Wu, and R. Jin, "Quantum sized gold nanoclusters with atomic precision," *Acc. Chem. Res.*, vol. 45, no. 9, pp. 1470–1479, 2012, doi: 10.1021/ar200331z.
[35] H. Xu and K. S. Suslick, "Water-soluble fluorescent silver nanoclusters," *Adv. Mater.*, vol. 22, no. 10, pp. 1078–1082, 2010, doi: 10.1002/adma.200904199.
[36] I. A. Ansari and R. Gree, "TEMPO-Catalyzed Aerobic Oxidation of Alcohols to Aldehydes and Ketones in Ionic Liquid [bmim][PF6]," *Org. Lett.*, vol. 4, no. 9, pp. 1507–1509, 2002, doi: 10.1021/ol025721c.
[37] S. E. Allen, R. R. Walvoord, R. Padilla-Salinas, and M. C. Kozlowski, "Aerobic copper-catalyzed organic reactions," *Chem. Rev.*, vol. 113, no. 8, pp. 6234–6458, 2013.
[38] P. J. Figiel, M. Leskelä, and T. Repo, "TEMPO-copper(II) diimine-catalysed oxidation of

benzylic alcohols in aqueous media," *Adv. Synth. Catal.*, vol. 349, no. 7, pp. 1173–1179, 2007, doi: 10.1002/adsc.200600505.
[39] J. March, *Advanced Organic Chemistry, Reactions, Mechanisms and Structure*, vol. 344. Wiley New York, 1966.
[40] L. Liang, G. Rao, H. L. Sun, and J. L. Zhang, "Aerobic oxidation of primary alcohols catalyzed by copper salts and catalytically active μ-hydroxyl-bridged trinuclear copper intermediate," *Adv. Synth. Catal.*, vol. 352, no. 14–15, pp. 2371–2377, 2010, doi: 10.1002/adsc.201000456.
[41] P. Lahtinen, J. U. Ahmad, E. Lankinen, P. Pihko, M. Leskelä, and T. Repo, "Organocatalyzed oxidation of alcohols to aldehydes with molecular oxygen," *J. Mol. Catal. A Chem.*, vol. 275, no. 1–2, pp. 228–232, 2007, doi: 10.1016/j.molcata.2007.06.001.
[42] T. V. Magdesieva *et al.*, "Copper(I) complexes with polymeric 2,2′-biquinoline-containing ligands as electrocatalysts for selective oxidation of the secondary hydroxy group in 3,24-dihydroxy-5β-cholane with oxygen," *Russ. J. Org. Chem.*, vol. 47, no. 1, pp. 62–65, 2011, doi: 10.1134/S1070428011010064.
[43] C. Jallabert and H. Riviere, "Activation de l'oxygene moleculaire par des sels de cuivre monovalent : transformation d'alcools en aldehydes par le systeme CuCl/amine/O2," *Tetrahedron Lett.*, vol. 18, no. 14, pp. 1215–1218, 1977, doi: 10.1016/S0040-4039(01)92978-8.
[44] C. Jallabert and H. Riviere, "Deshydrogenation d'alcools en composes carbonyles par le systeme CuCl/O2/Ligande," *Tetrahedron*, vol. 36, no. 9, pp. 1191–1194, 1980, doi: 10.1016/0040-4020(80)87017-7.
[45] N. Jiang and A. J. Ragauskas, "Copper(II)-catalyzed aerobic oxidation of primary alcohols to aldehydes in ionic liquid [bmpy]PF6," *Org. Lett.*, vol. 7, no. 17, pp. 3689–3692, 2005, doi: 10.1021/ol051293+.
[46] E. T. T. Kumpulainen and A. M. P. Koskinen, "Catalytic activity dependency on catalyst components in aerobic copper-TEMPO oxidation," *Chem. - A Eur. J.*, vol. 15, no. 41, pp. 10901–10911, 2009, doi: 10.1002/chem.200901245.
[47] P. Gamez and I. W. Arends, "CE; Reedijk, J.; Sheldon, RA," *Chem. Commun*, vol. 2414, 2003.
[48] K. Akagawa, S. Takigawa, E. Mano, and K. Kudo, "Sequential oxidation/asymmetric aldol reaction of primary alcohols by resin-supported catalysts," *Tetrahedron Lett.*, vol. 52, no. 7, pp. 770–773, 2011, doi: 10.1016/j.tetlet.2010.12.008.
[49] A. Dhakshinamoorthy, M. Alvaro, and H. Garcia, "Aerobic oxidation of benzylic alcohols catalyzed by metal-organic frameworks assisted by TEMPO," *ACS Catal.*, vol. 1, no. 1, pp. 48–53, 2011, doi: 10.1021/cs1000703.
[50] Y. Qi, Y. Luan, J. Yu, X. Peng, and G. Wang, "Nanoscaled copper metal-organic framework (MOF) based on carboxylate ligands as an efficient heterogeneous catalyst for aerobic epoxidation of olefins and oxidation of benzylic and allylic alcohols," *Chem. - A Eur. J.*, vol. 21, no. 4, pp. 1589–1597, 2015, doi: 10.1002/chem.201405685.
[51] I. Ibrahem *et al.*, "Copper Nanoparticles on Controlled Pore Glass and TEMPO for the Aerobic Oxidation of Alcohols," *ChemNanoMat*, vol. 4, no. 1, pp. 71–75, 2018, doi: 10.1002/cnma.201700309.
[52] S. Sakane *et al.*, "Catalytic Activity of Nonaggregating Cu Nanoparticles Supported in Pores of Zeolite for Aerobic Oxidation of Benzyl Alcohol," *ACS Omega*, vol. 9, no. 1, pp. 970–976, 2024, doi: 10.1021/acsomega.3c07156.

Supplementary Files

This is a list of supplementary files associated with this preprint. Click to download.

- supportinginformation.docx